Applied Catalysis B: Environmental 84 (2008) 545–551

Contents lists available at ScienceDirect

Applied Catalysis B: Environmental

journal homepage: www.elsevier.com/locate/apcatb

Excellent sulfur resistance of $Pt/BaO/CeO_2$ lean NO_x trap catalysts

Ja Hun Kwak, Do Heui Kim, János Szanyi, Charles H.F. Peden *

Institute for Interfacial Catalysis, Pacific Northwest National Laboratory, P.O. Box 999, Richland, WA 99354, United States

ARTICLE INFO

Article history:
Received 3 April 2008
Received in revised form 9 May 2008
Accepted 15 May 2008
Available online 23 May 2008

Keywords:
Ceria
LNT
Sulfur
Barium oxide
NO_x

ABSTRACT

In this work, we investigated the NO_x storage behavior of $Pt/BaO/CeO_2$ catalysts, especially in the presence of SO_2. High surface area CeO_2 (~110 m^2/g) with a rod like morphology was synthesized and used as a support. The $Pt/BaO/CeO_2$ sample demonstrated slightly higher NO_x uptake in the entire temperature range studied compared with $Pt/BaO/\gamma\text{-}Al_2O_3$. More importantly, this ceria-based catalyst showed higher sulfur tolerance than the alumina-based one. The time of complete NO_x uptake was maintained even after exposing the sample to ~3 g/L of SO_2. The same sulfur exposure, on the other hand, eliminated the complete NO_x uptake time on the alumina-based NO_x storage catalysts. TEM images show no evidence of either Pt sintering or BaS phase formation during reductive de-sulfation up to 600 °C on the ceria-based catalyst, while the same process over the alumina-based catalyst resulted in both a significant increase in the average Pt cluster size and the agglomeration of a newly formed BaS phase into large crystallites. XPS results revealed the presence of about five times more residual sulfur after reductive de-sulfation at 600 °C on the alumina-based catalysts in comparison with the ceria-based ones. All of these results strongly support that, besides their superior intrinsic NO_x uptake properties, ceria-based catalysts have (a) much higher sulfur tolerance and (b) excellent resistance against Pt sintering when they are compared to the widely used alumina-based catalysts.

1. Introduction

Reduction of NO_x (NO and NO_2) emissions from combustion processes, including vehicle engines, remains a challenge particularly for systems operating at high air-to-fuel ratios (so-called 'lean' combustion). The current automotive "3-way", precious metal-based catalytic converters are unable to selectively reduce NO_x with reductants (e.g., CO and residual unburned hydrocarbon) in the presence of excess O_2. In the last few years, worldwide environmental regulations regarding NO_x emissions from diesel engines (inherently operated 'lean') have become significantly more stringent, resulting in considerable research efforts to reduce NO_x under the highly oxidizing engine operation conditions. In recent years, alkali and alkaline earth oxide-based lean NO_x trap (LNT) catalysts (especially BaO/Al_2O_3) have been developed, and have shown promising activities for lean-NO_x reduction [1].

Even though LNTs are considered as one of the promising technologies for lean exhaust treatment, there are two major drawbacks for practical applications [2]. Both are closely related with sulfur in the diesel fuel and, therefore, difficult to avoid. One is the poisoning of the storage material by sulfur, and the other is thermal aging of the catalyst containing the precious metal (PM) component. Like NO, SO_2 in the oxygen rich exhaust undergoes similar chemical conversion (oxidation) on the PM component of the catalyst, and the thus formed SO_3 eventually gets stored as $BaSO_4$. Since $BaSO_4$ is thermodynamically more stable than $Ba(NO_3)_2$ [3], this process leads to the catalyst deactivation as the available storage sites are gradually consumed. Therefore, sulfur-poisoned catalysts require a high temperature regeneration process to convert $BaSO_4$ back into BaO or $BaCO_3$. During these de-sulfation processes, the effects of thermal aging on the catalyst, primarily Pt sintering and/or $BaAl_2O_4$ phase formation, have been demonstrated [4]. Thus, in order to develop a practically viable LNT catalyst, the issue of sulfur resistance needs to be addressed. To achieve this goal, two avenues can be envisioned: (1) development of a sulfur resistant NO_x storage system, and (2) development of an effective de-sulfation processes that do not adversely affect catalyst properties. Here, we follow the first path, by looking into the performance and sulfur resistance of a high surface area cerium oxide-supported, BaO-based NO_x storage system.

Ceria is an important component of currently used three-way catalysts by playing roles in both providing the oxygen storage capacity and maintaining high dispersions of the precious-metal components. In addition, ceria has been proposed as a support [5]

* Corresponding author. Tel.: +1 509 371 6501; fax: +1 509 371 6498.
E-mail address: chuck.peden@pnl.gov (Charles H.F. Peden).

0926-3373/$ – see front matter © 2008 Elsevier B.V. All rights reserved.
doi:10.1016/j.apcatb.2008.05.009

or a promoter [6] in LNT catalysts. One benefit of ceria-promoted catalysts is known to be the generation of hydrogen via water-gas shift and/or hydrocarbon steam-reforming reactions, which is expected to be used effectively during regeneration (reduction cycle) and de-sulfation [7]. Another role of ceria in LNT catalysts is related to sulfur resistance since it is known that SO_2 can be stored as cerium sulfate, which may aid in protecting the NO_x storage component (e.g., BaO) from sulfur poisoning [8].

Here, we report on the use of ceria as the catalyst support material *instead* of the widely used alumina. The ceria-based LNT catalysts were found to exhibit vastly improved sulfur resistance in comparison to the alumina-based counterparts. In addition, it is also demonstrated that a much smaller extent of Pt sintering occurs during the regeneration process, which can be important for long-term catalyst stability. We show that such behavior originates, at least in part, from the intimate interaction between Pt and CeO_2.

2. Experimental

High surface area CeO_2 was synthesized using a previously reported protocol [9]. After calcination in air at 350 °C for 4 h, the sample had a BET surface area of 110 m^2/g, with crystallites that exhibited a rod-like morphology with average diameter of ~5–10 nm and length of ~30–80 nm as estimated from TEM images. The 2 wt.% Pt/10 wt.% BaO/CeO_2 catalyst was prepared by conventional impregnation methods, with very similar procedures that we have used previously for the preparation of $Pt/Ba/Al_2O_3$, and described in detail elsewhere [10]. First, $Ba(NO_3)_2$ (Aldrich) was loaded to the desired level onto the pre-calcined CeO_2 support by repeated cycles of incipient wetness impregnation and room temperature drying. Then, the same incipient wetness impregnation and drying procedures were followed for the Pt loading, using an aqueous $Pt(NH_3)_4(NO_3)_2$ (Aldrich) solution. The dried sample was ultimately calcined at 500 °C for 2 h in flowing dry air. We also prepared a 2 wt.% Pt/20 wt.% BaO/Al_2O_3 catalyst for comparison using the same protocol. It is important to note that the 10 wt.% BaO on the ceria-supported catalyst (surface area ~110 m^2/g) has essentially the same amount of BaO per unit surface area as the 20 wt.% BaO on alumina-supported catalyst (surface area ~200 m^2/g).

The NO_x uptake measurements and sulfation/de-sulfation studies were performed in a fixed bed quartz reactor. Reactants consisted of a continuous flow of 200 ppm NO, 10% CO_2 and 10% H_2O balanced with He with either rich (1330 ppm C_3H_6, 4% CO and 1.33% H_2) or lean (12% O_2) gas added over 0.1167 g of catalyst at a total flow rate of 300 cm^3/min. We emphasize that using the same weight of catalysts in these experiments, means that the ceria-based material contains only half of the total amount of BaO in the reactor as compared to the alumina-based catalyst. As noted above, even though the estimated total surface coverage of BaO is the same in both catalysts, the weight % (and, thus, molar %) is lower as a direct result of the lower surface area of the ceria-based material. All gases were

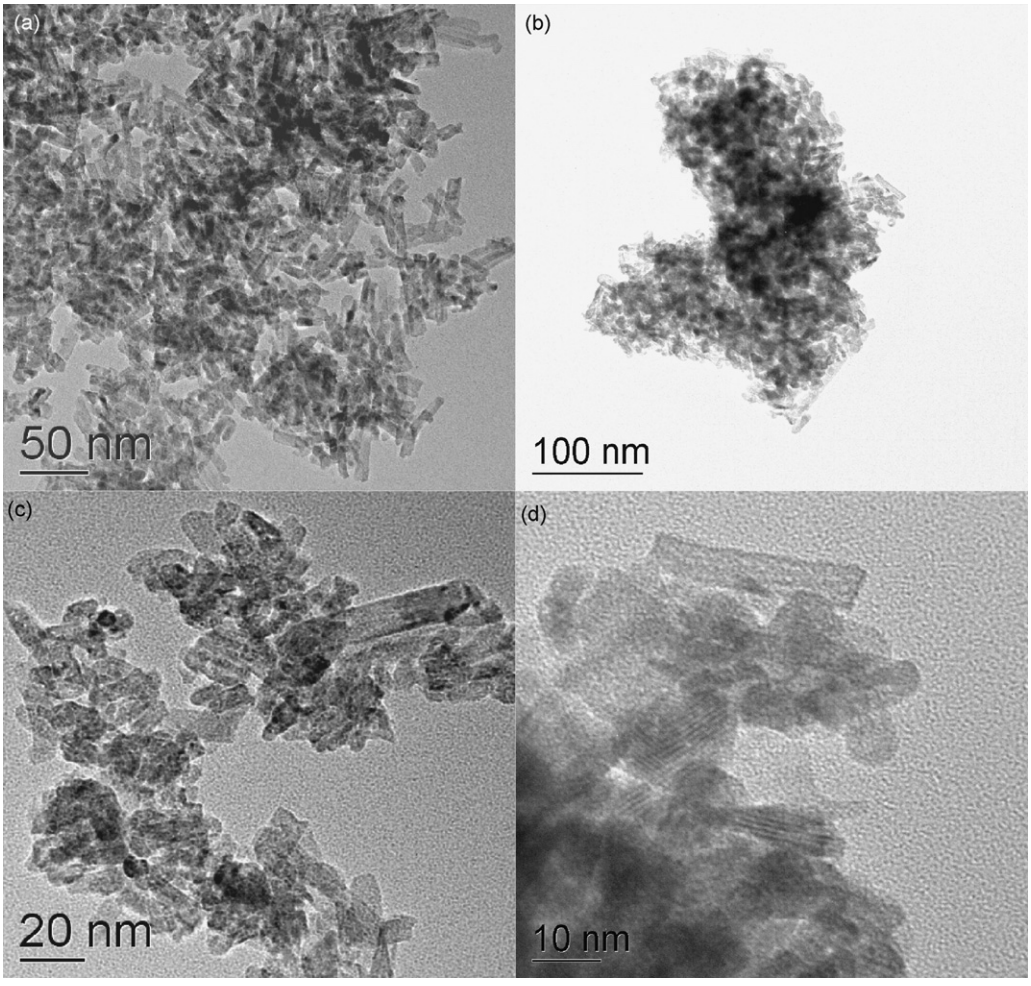

Fig. 1. TEM images for synthesized CeO_2 (a and c) after calcined at 350 °C and $Pt/BaO/CeO_2$ (b and d) after calcined at 500 °C.

controlled by mass flow controllers (Brooks). The NO_x concentration at the inlet (~200 ppm) and outlet of the reactor were measured with a chemiluminescence NO_x analyzer (Thermo Electron, 42C). Detailed reaction conditions used for performance measurements in this study have been described in our previous publication [10]. Briefly, NO_x uptake was measured after four complete lean/rich (4 min/1 min) cycles were introduced. The NO_x uptake was defined as the difference between the amount of NO_x passed through the catalyst bed unreacted and the amount of inlet NO_x during a lean cycle of 30 min. NO_x uptakes were measured at 250, 300, 350 and 400 °C.

After the NO_x uptake measurement in the absence of SO_2, sulfation was carried out by treating the sample at 250 °C with 25 ppm SO_2 in the lean gas mixture (see above) for 3 h. The total amount of SO_2 passing through the catalyst bed during sulfation was 0.055 m mol. After sulfation, the NO_x uptake was measured at a 250 °C catalyst bed temperature. A final NO_x uptake measurement was also carried out at 250 °C, after the sulfated sample was treated with a rich gas mixture for 5 min at 600 °C in order to remove (at least partially) the sulfur. Post-reaction samples were then collected for the XPS and TEM analysis.

X-ray photoelectron spectroscopy (XPS) experiments were carried out for post-reaction samples in the analysis chamber of a Physical Electronics Instruments Quantum 2000, using Al Kα X-rays and a pass energy of 71 eV. The position and intensity of the Al 2s peak at 119.2 eV was used as reference.

TEM micrographs were obtained for the fresh and post-reaction samples using a JEOL 2010 high-resolution analytical electron microscope operating at 200 kV electron beam voltage. An energy-dispersive X-ray (EDS) analyzer was used for elemental analysis. Powder samples were dispersed onto a carbon-coated copper grid for TEM/EDS analysis.

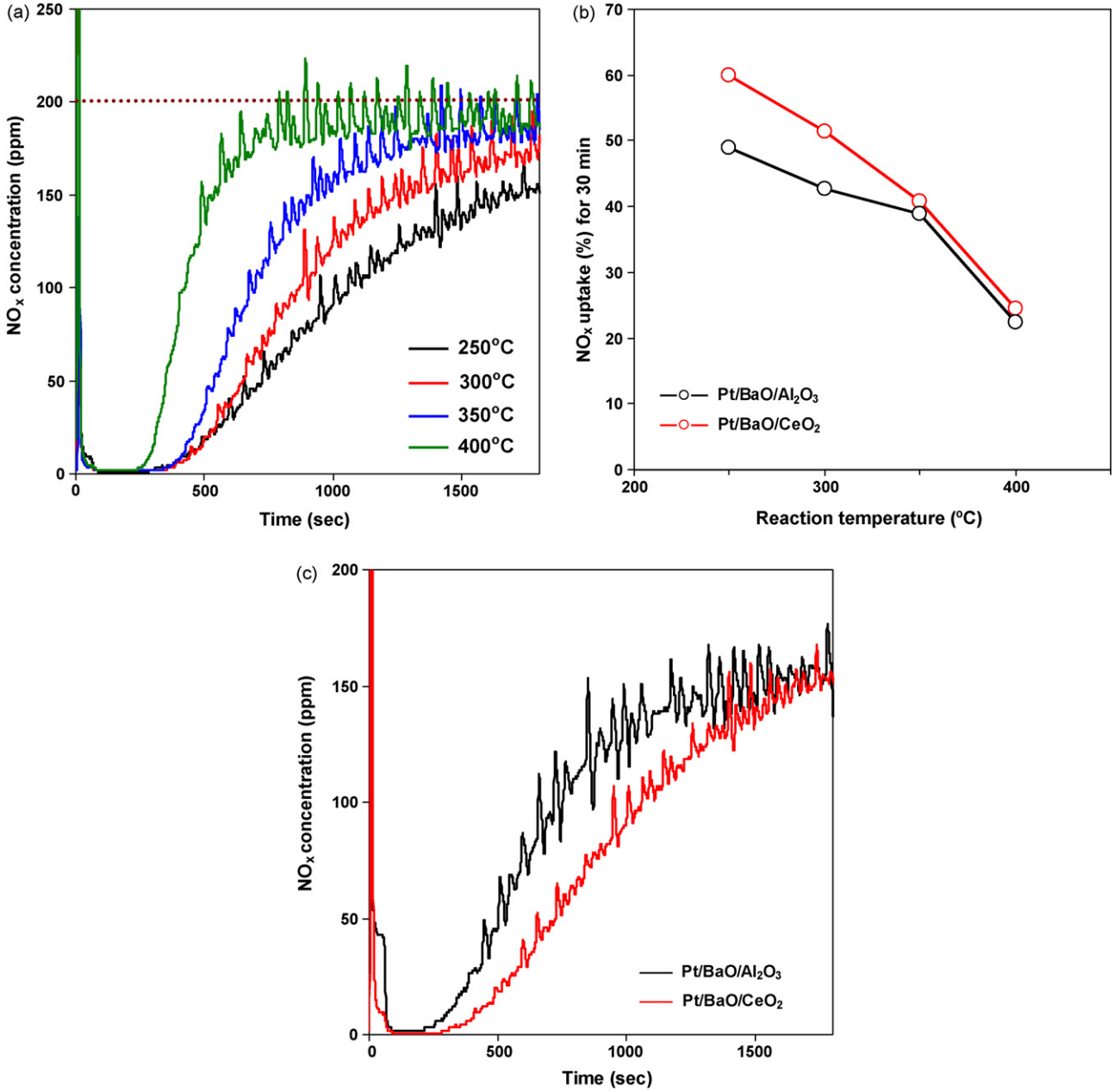

Fig. 2. NO_x uptake profiles for various temperatures for 2% Pt/10% BaO/CeO_2 (a), comparison of NO_x uptake (%) of 2% Pt/10% BaO/CeO_2 and 2% Pt/20% BaO/Al_2O_3 (b), and NO_x uptake profile at 250 °C for 2% Pt/10% CeO_2 and 2% Pt/20% BaO/Al_2O_3 samples (c).

3. Results and discussion

Fig. 1(a) and (c) show TEM images of as-synthesized high surface area CeO_2. CeO_2 synthesized and then calcined at 350 °C shows a nano-rod morphology with particles ~5–10 nm in diameter and 30–80 nm in length. The surface area estimated from BET measurements is ~110 m^2/g which is consistent with the preparation method used here, and reported previously [9]. Fig. 1(b) and (d) show representative TEM images of a fully formulated, calcined $Pt/BaO/CeO_2$ sample. Comparing the images obtained from the ceria support alone to those of the fully formulated catalyst, it is evident that they exhibit the same morphologies. XRD analysis of the crystalline phases present (not shown in this paper) also indicates that there are no changes in the ceria crystallite size during the Pt and Ba loading and the subsequent calcination at 500 °C in air. These results confirm the excellent stability of the ceria support under these catalyst synthesis conditions, also consistent with the results of a previous report [9]. Interestingly, no Pt or Ba clusters can be seen in these TEM images of $Pt/BaO/CeO_2$. In our previous studies on $Pt/BaO/Al_2O_3$, NO_x storage catalysts [10], we could readily observe Pt clusters with 1–2 nm average size. However, as shown in Fig. 1(d) (and in many other images not shown here), we could not find any evidence of Pt cluster formation on these ceria-based catalysts. The TEM results suggest that very small size Pt clusters formed on this ceria supports. The existence of strong metal support interaction between group VIII metals and reducible transition metal oxide supports, such as CeO_2, TiO_2, etc., is well known [11,12]. We believe that the strong interaction between Pt and the CeO_2 support in our catalysts is critical for obtaining this high dispersion of Pt clusters.

Fig. 2(a) shows the NO_x uptake profiles over the $Pt/BaO/CeO_2$ catalyst at various temperatures (250–400 °C). These NO_x uptake profiles are very similar to those we have seen for $Pt/BaO/Al_2O_3$ catalysts in our previous studies [9]. However, ceria-based

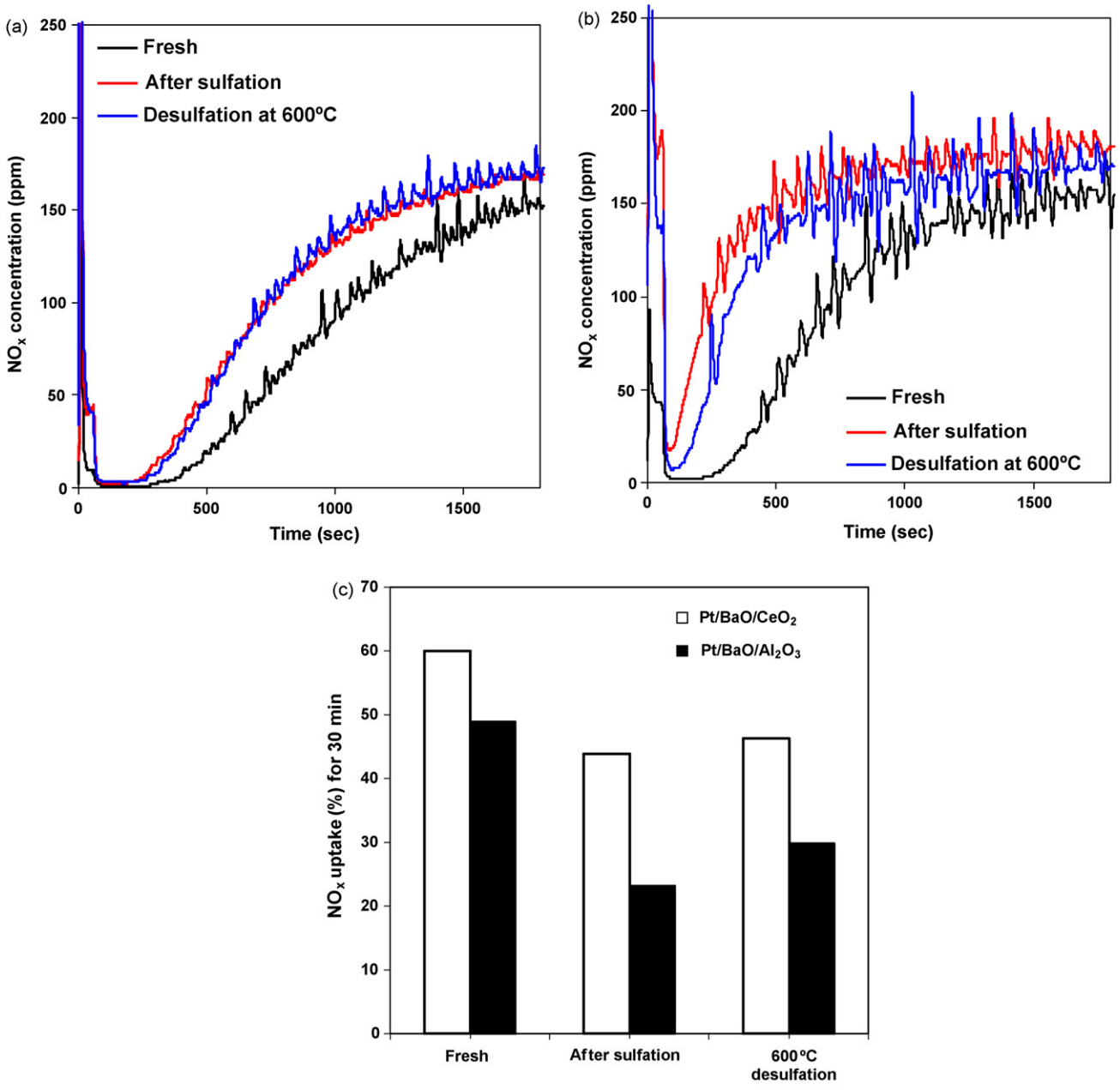

Fig. 3. NO_x uptake profile changes by sulfation and de-sulfation for $Pt/BaO/CeO_2$ (a) and $Pt/BaO/Al_2O_3$ (b), and NO_x uptake (%) for 30 min (c).

catalysts exhibit slightly higher NO_x uptake (%) over the entire temperature range studied (Fig. 2(b)). For example, the NO_x uptake at 250 °C for the ceria-based catalyst is ~60% which is significantly higher than the 49% measured for the alumina-based catalyst. Note that the difference in NO_x uptake between the ceria- and alumina-based catalysts decreases with increasing reactor temperature, and they are very similar (~24% versus ~22%) at the highest temperature of this study (400 °C). In Fig. 2(c), the NO_x uptake profiles of the 2% Pt/20% BaO/Al_2O_3 and 2% Pt/10% BaO/CeO_2 are compared at 250 °C, where the highest NO_x uptakes were obtained for both catalysts. This high activity of the ceria-based catalyst is surprising since this catalyst contains only half the total amount of storage material (barium oxide) in comparison to the alumina-supported one (see Section 2). This observation strongly implies that the ceria support plays a critical role in improving the efficiency of barium oxide in storing NO_x species.

A very important observation from the comparative NO_x uptake curves shown in Fig. 2(c) is the significantly longer complete uptake time on the ceria-based catalyst, again noting that the ceria-based catalyst contains only half the BaO loading. In our previous report [10], this complete uptake time was interpreted as the result of continuous NO_2 spillover from Pt to the neighboring, empty barium oxide sites. This process is characterized by fast and complete NO_x uptake, and becomes diffusion-limited as the availability of BaO sites in close proximity to Pt sites decreases. This implies that the time period in which complete NO_x uptake occurs is controlled by the number of BaO entities in direct contact with Pt clusters, and not by the overall BaO coverage on the support. As the surface area of ceria is approximately half of that of alumina, the BaO coverage on the ceria support (assuming an even BaO distribution on the surface) is similar to that on alumina. If the surface coverage of BaO is the same for both catalysts, then the complete NO_x uptake time should be primarily controlled by the number of Pt clusters, which, in turn, determines the effective Pt/BaO interface area where facile NO_2 spillover can take place. Thus, the longer complete NO_x uptake time for $Pt/BaO/CeO_2$ sample can be explained by a higher dispersion of Pt on the ceria support. This interpretation is consistent with TEM results that evidenced smaller Pt clusters formed on ceria-based catalysts than on alumina-based ones.

In order to investigate the effect of sulfur on both the ceria- and alumina-based catalysts, we first exposed both catalysts at 250 °C to the same amount of SO_2, and then measured the NO_x uptake at the same temperature. Panels (a) and (b) of Fig. 3 show the NO_x uptake profiles at 250 °C before and after sulfur treatment for the ceria- and alumina-based catalysts, respectively. The NO_x uptake capabilities of both catalysts significantly decreased as a result of their exposure to SO_2. However, the alumina-based catalyst exhibits a much higher extent of deactivation than the ceria-based one. Variation in NO_x uptake (for a 30 min lean uptake) by sulfation/de-sulfation treatment is summarized in Fig. 3(c) for both catalysts. After SO_2 treatment, NO_x uptake of the alumina-based catalyst was reduced from 48% to 23% while on the ceria-based catalyst it decreased from 60% to 43%. The overall NO_x uptake recovered only partially after reductive de-sulfation at 600 °C; it improved by 3% for $Pt/BaO/CeO_2$ and by 6% for $Pt/BaO/Al_2O_3$. Also of interest is that the changes in the NO_x uptake profiles as a result of SO_2 treatment were very different for the two catalysts, especially with respect to variations in the complete NO_x uptake times. After SO_2 exposure, the time period of complete NO_x uptake on the alumina-based catalyst completely disappeared and, at the start of the NO_x uptake experiment, NO_x broke through immediately and its concentration never dropped below 15 ppm. In contrast, the ceria-based catalyst showed only a small change in the complete NO_x uptake time; it was 8 min on the fresh sample (before SO_2 exposure) and 6 min after sulfur treatment to reach a NO_x level of 10% of the input value.

The sulfur-poisoning mechanism on $Pt/BaO/Al_2O_3$ catalysts is generally accepted to be initiated by the oxidation of SO_2 on the metallic Pt particles, followed by a spillover of the thus produced SO_3 to the vicinal barium phase to form barium sulfate near the Pt clusters [13]. Therefore, the results obtained on the $Pt/BaO/Al_2O_3$ catalyst after sulfur treatment can be interpreted as the elimination of available barium oxide sites for NO_x adsorption near the Pt clusters. The barium oxide sites in intimate contact with the Pt particles are then completely occupied by sulfates; therefore, NO_x storage by NO_2 spillover (fast or complete NO_x uptake) is completely eliminated and no complete NO_x uptake period is observed. On the other hand, very interestingly, the ceria-based catalyst exhibits a significantly long complete NO_x uptake time even after the same SO_2 exposure as the alumina-based catalyst (the complete NO_x uptake time only decreased by about 25%). This indicates that the active BaO phase near the Pt clusters remains available for NO_x storage even after SO_2 exposure. The sulfur resistance of this ceria-based catalyst is remarkable, and is potentially very important since the practical application of alumina-based NSR catalysts is hindered primarily by their susceptibility toward sulfur poisoning.

A number of possible explanations can be suggested for the excellent resistance against sulfur poisoning of these ceria-based catalyst discussed here. One is the storage of sulfur-containing species as cerium sulfate rather than as barium sulfate. The role of ceria as a promoter to improve sulfur resistance of $Pt/BaO/Al_2O_3$ catalyst systems has been proposed [8], and explained by the sulfation of the ceria additive rather than the BaO phase. This may occur due to the direct formation of sulfates on the ceria additive as a result of the reaction between labile (active) oxygen present on the ceria under lean conditions and SO_2. The other possible explanation is the lower amount of overall sulfur uptake due to the high dispersion of Pt particles (small average Pt particle size) on the CeO_2 support. The rate of NO oxidation to NO_2 has been shown to increase with increasing average Pt cluster size [14], perhaps due to the higher resistance of the larger Pt cluster to oxidation (i.e., PtO formation). By the same analogy, the small Pt clusters formed on the ceria surface are believed to be less active for the oxidation of SO_2 to SO_3, which would ultimately lead to a lowered formation of barium sulfate.

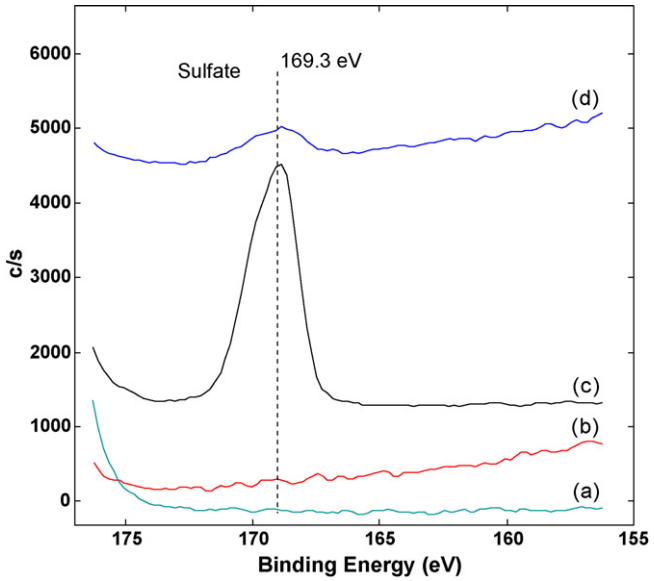

Fig. 4. XPS data of sulfur 2p data for fresh and after de-sulfation at 600 °C of $Pt/BaO/CeO_2$ (b and d) and $Pt/BaO/Al_2O_3$ (a and c).

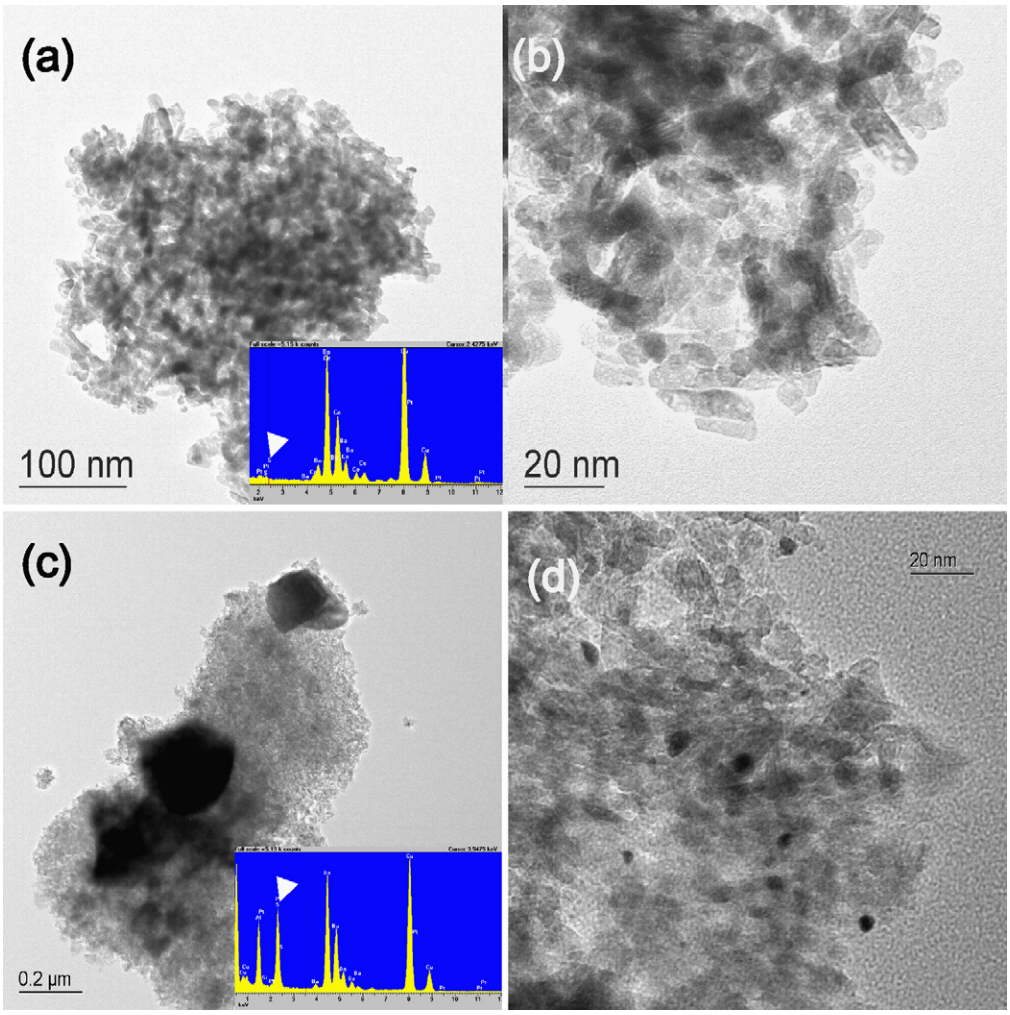

Fig. 5. TEM images for $Pt/BaO/CeO_2$ (a and b) and $Pt/BaO/Al_2O_3$ (c and d) after de-sulfation at 600 °C.

To obtain information relevant to the mechanism for reduced sulfur poisoning of the ceria-based catalysts, we performed XPS and TEM/EDS analysis on both the Al_2O_3- and CeO_2-supported catalysts after reductive de-sulfation at 600 °C. XPS results shown in Fig. 4 demonstrate that a significantly lower level of residual sulfur is present on the ceria-based catalyst after reductive de-sulfation. The amount of residual sulfur estimated from XPS data, for $Pt/BaO/CeO_2$ (Fig. 4(d)) is ~0.75% while that for $Pt/BaO/Al_2O_3$ (Fig. 4(c)) is ~3.38%. TEM/EDS analysis, shown in Fig. 5, also show a significantly smaller residual sulfur level for the ceria-based catalyst. These results also provide information about the morphology of the remaining SO_x-containing particles. The TEM images of a post-reaction $Pt/BaO/Al_2O_3$ sample (Fig. 5(c) and (d)) showed the agglomeration of large barium-sulfide particles (see especially panel (c) in Fig. 5), with the identity of these agglomerates confirmed by a strong sulfur EDS signal (inset). We concluded in a recent study [15] that, at high barium loadings (around 20 wt.%), reductive de-sulfation mostly transformed $BaSO_4$ phases into BaS, with very little sulfur actually removed. In contrast, over the post-reaction ceria-supported sample no evidence for the agglomeration of barium-sulfide particles was seen (e.g., compare panels (a) and (c) in Fig. 5). In addition, EDS analysis (not shown) indicated only a very small amount of residual sulfur on the ceria-supported sample in agreement with the XPS results discussed above. During the temperature programmed reductive de-sulfation process no significant difference in the amount of sulfur-related products (primarily H_2S) was observed for these two catalysts by mass spectrometry. In fact, the H_2S evolved during the reduction process was, if anything, even lower for the ceria-based catalyst. Therefore, based on the results of the XPS and TEM-EDS analysis, we conclude that the sulfur resistance of the ceria-based catalyst is not due primarily to the sulfur storage on cerium oxide phase. Instead, we propose that the $Pt/BaO/CeO_2$ catalyst is intrinsically more sulfur resistant due to the suppression of SO_2 oxidation to SO_3 (the prerequisite for Ba-sulfate formation) over the smaller Pt particles present in this catalyst. In addition to the amount of residual sulfur present, there is also a significant difference in the extent of sintering of the Pt particles occurring during reductive de-sulfation at 600 °C over these two catalysts. In the high resolution, TEM image of the ceria-supported sample (panel (b) in Fig. 5) no Pt particles can be distinguished. By contrast, on the alumina-supported catalyst ~5 nm Pt clusters were formed (panel (d) in Fig. 5). This result agrees well with that of Casapu et al. [16] in that Pt Pt-Ba/CeO_2 maintained its small particle size during reductive treatments up to 800 °C. On the other hand, Pt particles sinter faster even at lower temperatures over Al_2O_3-supported catalysts due to a weaker interaction between Pt and the support material [17]. These results suggest a secondary advantage that the use of ceria-based catalysts provides; notably, the suppression of Pt sintering during the de-

sulfation at 600 °C, and thereby maintaining good catalytic activity.

4. Conclusions

In summary, the Pt-BaO/CeO_2 LNT catalyst sample demonstrates longer complete NO_x uptake time and a higher amount of total NO_x stored than the alumina-supported one even at a lower barium loading. From the practical point of view, these ceria-based catalysts exhibit a remarkably lower extent of sulfur poisoning and a significantly higher resistance against Pt sintering during high temperature reductive de-sulfation processes in comparison to the alumina-based ones. Thus, these results suggest an approach to circumventing the two major drawbacks of the alumina-based LNT catalysts by the application of the high surface area ceria support.

Acknowledgements

Financial support was provided by the U.S. Department of Energy (DOE), Office of Freedom Car and Vehicle Technologies. The work was performed in the Environmental Molecular Sciences Laboratory (EMSL) at the Pacific Northwest National Laboratory (PNNL). The EMSL is a national scientific user facility and supported by the U.S. DOE's Office of Biological and Environmental Research. PNNL is a multi-program national laboratory operated for the U.S. Department of Energy by Battelle Memorial Institute under Contract DE-AC06-76RLO 1830.

References

[1] N. Takahashi, H. Shinjoh, T. Iijima, T. Suzuki, K. Yamazaki, K. Yokota, H. Suzuki, N. Miyoshi, S. Matsumoto, T. Tanizawa, T. Tanaka, S. Tateishi, K. Kasahara, Catalysis Today 27 (1996) 63–69.
[2] W.S. Epling, L.E. Campbell, A. Yezerets, N.W. Currier, J.E. Parks, Catalysis Reviews—Science And Engineering 46 (2004) 163–245.
[3] L. Lietti, P. Forzatti, I. Nova, E. Tronconi, Journal of Catalysis 204 (2001) 175–191.
[4] D.H. Kim, Y.H. Chin, G.G. Muntean, A. Yezeretz, N.W. Currier, W.S. Epling, H.Y. Chen, H. Hess, C.H.F. Peden, Industrial & Engineering Chemistry Research 45 (2006) 8815–8821.
[5] M. Casapu, J.D. Grunwaldt, M. Maciejewski, M. Wittrock, U. Gobel, A. Baiker, Applied Catalysis B—Environmental 63 (2006) 232–242.
[6] F. Rohr, S.D. Peter, E. Lox, M. Kogel, A. Sassi, L. Juste, C. Rigaudeau, G. Belot, P. Gelin, M. Primet, Applied Catalysis B—Environmental 56 (2005) 201–212.
[7] G. Jacobs, L. Williams, U. Graham, G.A. Thomas, D.E. Sparks, B.H. Davis, Applied Catalysis A—General 252 (2003) 107–118.
[8] M.A. Peralta, V.G. Milt, L.M. Cornaglia, C.A. Querini, Journal of Catalysis 242 (2006) 118–130.
[9] K.B. Zhou, X. Wang, X.M. Sun, Q. Peng, Y.D. Li, Journal of Catalysis 229 (2005) 206–212.
[10] J.H. Kwak, D.H. Kim, T. Szailer, C.H.F. Peden, J. Szanyi, Catalysis Letters 111 (2006) 119–126.
[11] S.J. Tauster, S.C. Fung, R.T.K. Baker, J.A. Horsley, Science 211 (1981) 1121–1125.
[12] S.J. Tauster, S.C. Fung, R.L. Garten, Journal of the American Chemical Society 100 (1978) 170–175.
[13] S. Matsumoto, Y. Ikeda, H. Suzuki, M. Ogai, N. Miyoshi, Applied Catalysis B—Environmental 25 (2000) 115–124.
[14] L. Olsson, E. Fridell, Journal of Catalysis 210 (2002) 340–353.
[15] D.H. Kim, J. Szanyi, J.H. Kwak, T. Szailer, J. Hanson, C.M. Wang, C.H.F. Peden, Journal of Physical Chemistry B 110 (2006) 10441–10448.
[16] M. Casapu, J.D. Grunwaldt, M. Maciejewski, A. Baiker, S. Eckhoff, U. Gobel, M. Wittrock, Journal of Catalysis 251 (2007) 28–38.
[17] Y. Nagai, T. Hirabayashi, K. Dohmae, N. Takagi, T. Minami, H. Shinjoh, S. Matsumoto, Journal of Catalysis 242 (2006) 103–109.